Effect of localized oxygen functionalization on the conductance of metallic carbon nanotubes

M. K. Ashraf,[1,*] Nicolas A. Bruque,[1,†] Rajeev R. Pandey,[2] Philip G. Collins,[3] and Roger K. Lake[1]
[1]*Department of Electrical Engineering, University of California–Riverside, Riverside, California 92521, USA*
[2]*Department of Chemistry, University of the Pacific, Stockton, California 95211, USA*
[3]*Department of Physics and Astronomy, University of California–Irvine, Irvine, California 92697, USA*
(Received 9 September 2008; revised manuscript received 28 January 2009; published 20 March 2009)

A comprehensive study of the effect of covalent oxygen attachment on the transmission and conductance of armchair and metallic zigzag carbon nanotubes (CNTs) is presented. In both armchair and zigzag CNTs covalent oxygen attachment favors an ether-type bond in which the C-C bond breaks. Oxygen atoms attached on the CNT surface within the same carbon ring on parallel bonds are energetically more stable than well-separated attachments. In an armchair CNT, oxygen attachment favors the C-C bonds orthogonal to the CNT axis. *Cooperative* addition propagates axially along parallel orthogonal bonds. In a zigzag CNT, oxygen attachment prefers the slanted bond, and cooperative addition propagates spirally along parallel slanted bonds. Closely spaced oxygen attachment on the armchair and zigzag CNT surfaces causes a dip in transmission symmetrically away from the Fermi level at the turn-on of the first excited modes. For both armchair and zigzag CNTs, as more oxygen atoms are placed in close proximity, their levels interact and split and move closer to the Fermi level which results in broader dips in transmission closer to the Fermi level. The transmission of armchair CNTs near the charge-neutral Fermi level is relatively insensitive to a group of localized oxygen atoms compared to that of metallic zigzag CNTs. A clustered group of oxygen atoms covalently attached to a single-walled metallic zigzag CNT can result in a 1 order of magnitude drop in transmission that is asymmetric with respect to the Fermi energy resulting in a qualitative resemblance to conductance versus gate voltage curves observed experimentally. The covalent attachment of a single oxygen atom in any configuration, on either, an armchair, or zigzag metallic CNT does not give rise to a large change in conductance. Calculations use density-functional theory combined with nonequilibrium Green's functions.

DOI: 10.1103/PhysRevB.79.115428 PACS number(s): 73.63.Fg, 31.15.ae, 73.22.−f

I. INTRODUCTION

Carbon nanotubes (CNTs) are a candidate for future nanoelectronics applications due to their exotic electronic properties. Having their size comparable to the chemically active molecules, they can provide direct access to the chemical environment and provide information about single molecule events in chemical reactions and biological processes.[1] They are a candidate for elements of molecular level sensor devices.[2,3] The electrical detection of a single chemical attachment is regarded as a promising tool for future metrology applications.[4]

The recent report describing the controlled addition of one or several localized molecular attachments on a CNT surface[5,6] provides the focus for this paper. One or several localized molecular attachments on a CNT were shown to significantly alter the conductance of the CNTs and even change the conductance versus gate voltage response of metallic CNTs to resemble that of *p*-type semiconducting CNTs.[5] We pose the question, "Can one or several localized covalently attached oxygen atoms significantly alter the conductance of a metallic CNT as observed experimentally?" We describe the results of a comprehensive set of simulations investigating the effect of covalently attached oxygen atoms on the CNT transmission and conductance.

Interest in CNT functionalization began when Chen *et al.*[7] reported the first covalent functionalization of CNTs by nitric acid treatment. They demonstrated that covalent addition of dichlorocarbene to the sidewalls of CNTs can transform a metallic CNT to a semiconducting one when the Cl/C concentration ratio reaches around 25%.[8,9] Theoretical studies followed the experiments and revealed many surprising phenomena.[10,11] The effect of functionalization on the energy bands and transport properties has been studied using various density-functional theory (DFT) methods.[12–17] One result that was established through these studies is that monovalent atoms when attached on the sidewall of CNTs break the sp^2 network at the site, and the π bond at the C attachment site transforms to a sigma bond.[16] This bonding pattern affects the transmission spectra close to the Fermi level, and about 25% adatom to CNT C ratio can completely destroy the conducting properties of CNTs.[11] Covalent attachment of divalent atoms, on the other hand, retains the local sp^2 network of the pristine CNT and moderately perturb the conductance. Even at 25% concentration, the conductance only drops by a factor of 2, and the CNT remains conductive. These theoretical studies concentrated on adatoms distributed randomly over the CNT surface.

Only a truly random process such as irradiation will introduce sparse, randomly distributed functional sites. When an atom attaches to a CNT, it perturbs nearby bonds and enhances the reactivity of adjacent sites. It then becomes energetically favorable for the next addition to attach in close proximity to the initial adatom. This type of cooperative behavior in which consecutive additions occur in close proximity in a cooperative pattern is referred to as *cooperative* addition. Yumura *et al.*[18] reported an example of cooperative behavior in divalent group attachment on CNTs. They found cooperative behavior among functionalization groups only when the first group was attached endohedrally, on the inside of the CNT surface. They did not find any cooperative effect

when the first group was attached exohedrally, on the outside of the CNT surface. The absence of cooperative behavior in exohedral attachment could be due to the steric hindrance caused by the larger dichlorocarbene functional groups used in the study. Most relevant to this work is the observation of cooperative addition in oxygen adsorption on graphite surfaces by Li *et al.*[19] With two oxygen atoms on a graphite surface, energy is minimized when two oxygen atoms are placed on parallel bonds of the six membered carbon ring. For a higher number of adatoms, the atoms sit side by side and form a line. This concerted alignment is believed to be the reason for breaking of the graphite structure and the cutting of the CNTs when oxidized. We find similar cooperative attachment patterns in CNTs. For two oxygen atoms on a CNT, the energy is also minimized when they attach across two parallel bonds of a six-membered carbon ring. The most energetically favorable geometry for multiple oxygen attachments is axial alignment on armchair CNTs and spiral alignment on zigzag CNTs along parallel C-C bonds.

Of particular interest is the recent experimental report of localized, single-molecule, covalent attachments on the CNT surface causing a qualitative change in the current versus gate voltage response of metallic CNTs.[5,20] The selective electrochemical deposition used in the experiment indicates that the functionalization is limited to a few sites over a narrow region on the CNT surface. For multiple attachments, it is highly probable that the adatoms are attached in a cooperative fashion. Based on the experimental redox chemistry, it is believed that hydroxide or oxygen in an epoxide or ether configuration is the species that is causing the conductance modulation.

Motivated by these recent experimental observations, we study the transport properties of CNTs locally functionalized with oxygen. We investigate if there is any local functionalization possible that could cause a significant change in the conductance and a qualitative change in the conductance versus gate voltage response of a metallic CNT. Both armchair and metallic zigzag CNTs are considered in a study of the possible structures and their transmission and conductance.

II. STRUCTURE AND THEORY

The calculation of the transmission uses DFT coupled with a nonequilibrium Green's function (NEGF) algorithm. Details of the DFT-based method can be found in Refs. 21–25, and the NEGF approach is described in Ref. 26. An overview of the main features is given below.

The DFT approach is implemented in a self-consistent, *ab initio*, tight-binding molecular dynamics code called FIREBALL. Separable, nonlocal Troullier-Martins pseudopotentials and the BLYP exchange-correlation functional are used.[27–29] At the heart of the method is a self-consistent generalization of the Harris-Foulkes energy functional[30,31] known as DOGS named after the original authors.[22,23,25] In the self-consistent evaluation of the total energy, the density is based on the sum of confined atomiclike densities $\rho(\mathbf{r}) = \Sigma_i n_i |\phi_i(\mathbf{r}-\mathbf{R}_i)|^2$, where n_i is the occupation of orbital ϕ_i centered at $\mathbf{R}_i$.[22] The orbitals, which are slightly excited pseudoatomic wave functions, serve as the basis functions for solving the one-electron Schrödinger equation. They are slightly excited due to hard wall boundary conditions imposed at certain radial cutoffs r_c which are determined by an excitation energy of approximately 2.0 eV, thereby preserving the chemical bonding trends. In this work, a double numerical basis set is used and the chosen cutoff values are as follows. For carbon, $r_c^{2s}=4.4$ Å for the *s*-orbital wave function and a $r_c^{2p}=4.8$ Å for the $p_{x,y,z}$-orbital wave functions. For oxygen $r_c^{2s}=3.7$ Å for the *s*-orbital wave function and a $r_c^{2p}=4.1$ Å for the $p_{x,y,z}$-orbital wave functions. All two and three center integrals are tabulated as functions of interatomic distances in advance and placed on interpolation grids. Molecular-dynamics simulations are performed by looking up the integrals from the interpolation grids. Structures are relaxed until all Cartesian forces on the atoms are <0.05 eV Å^{-1}. A Fermi smearing temperature of 50 K and a self-consistent convergence factor of 10^{-5} are used. The one-dimensional (1D) Brillouin zone is sampled with 32 *k* points during optimization.

The Hamiltonian matrix elements of the relaxed structure are used in the NEGF algorithm to calculate the surface self-energies, the Green's function of the device, and the resulting transmission. To calculate room-temperature conductance, we take the derivative of the current with respect to the voltage. The transmission spectrum, $T(E)$, and the conductance, G, are calculated from the standard Green's-function expressions,

$$T(E) = \mathrm{tr}\{\Gamma_{1,1} G^R_{1,N} \Gamma_{N,N} G^R_{1,N}\}, \tag{1}$$

and

$$G = \frac{\partial I}{\partial V} = \frac{2e}{\hbar} \int \frac{dE}{2\pi} T(E) \left(- \frac{\partial f(E-E_f)}{\partial E} \right). \tag{2}$$

The indices 1 and N in Eq. (1) indicate the first and last block layer of the CNT, respectively. In Eq. (2), $f(E)$ is the Fermi function, and E_f is the Fermi energy. Calculations of G vs E_F are performed using the $T(E)$ calculated from the globally charge-neutral structure and sweeping E_F in Eq. (2) to create $G(E_F)$. Further details of our approach can be found in Ref. 26.

Spin-polarized DFT calculations[32] have shown that with oxygen functionalized (8,0) CNTs, the spin singlet configuration is preferred over triplet configuration by about 29 kcal/mol on the outer wall of the CNT. Similar results were obtained for oxygen addition on analogs of nanotube caps.[33] We perform spin-unpolarized DFT calculations.

The CNT model consists of a functionalized central region otherwise known as the device region. The device region consists of 18–24 atomic layers for an armchair CNT and 20–24 atomic layers for a zigzag CNT. Previous studies show that the energy configuration of functionalized CNTs is significantly influenced by their diameter.[14] Therefore, we take a (7,7) armchair and (12,0) zigzag CNT with diameter ~ 1 nm to match the CNTs used in the experiment.[5]

For verification, we also relaxed one CNT structure containing one oxygen atom on the orthogonal bond of an armchair CNT using GAUSSIAN03 (Ref. 34) and the Vienna *ab initio* simulation package (VASP) (Ref. 35) in addition to

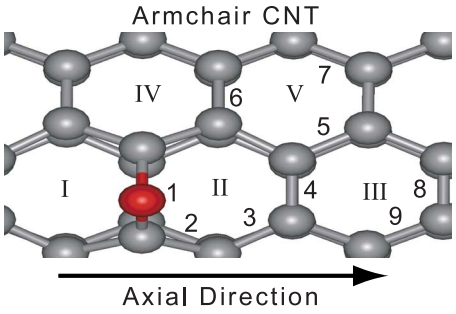

FIG. 1. (Color online) Section of an armchair CNT illustrating the two types of bonds, orthogonal and slanted. Arabic numerals label the bonds and Roman numerals label the rings. The red atom at bond 1 is the oxygen atom. "Orthogonal" denotes the bonds that are orthogonal to the axial direction such as bonds 1, 4, 6, and 8. "Slanted" denotes the other type of bond such as 2, 3, 5, 7, and 9.

FIREBALL. Such a geometry is shown in Fig. 1. The Gaussian relaxation was performed using the PM3 semiempirical model.[36,37] The relaxation convergence criteria was set to 4.5×10^{-4} eV/A. The VASP calculation employed the projector augmented wave (PAW) method with the generalized gradient approximation (GGA) Perdew-Burke-Ernzerhof (PBE) (Ref. 38) exchange correlation functional. We applied a plane-wave basis cutoff at 400 eV and an augmented charge cutoff of 600 eV. The CNT system was sampled with a $11\times1\times1$ irreducible k-point grid with an energy convergence criteria of less than 10^{-4} eV. The relaxation convergence criterion was set to 10^{-2} eV/A. All of the simulations resulted in an ether configuration of the C-O-C bond in which the original C-C bond is broken. Table I summarizes the bond lengths and angles obtained. The C-C (orthogonal) and C-C (slanted) bonds are taken from the bonds on the CNT surface farthest from the ether. A systematic variation occurs in the C-C bond lengths predicted by the three different simulations. However, the ratio of the C-C distance in the ether to C-C distance of the pristine CNT is consistent among the three different simulations. This *bond opening ratio* (BOR) will be used as a metric for describing the C-C bond opening and closing resulting from different attachment sites and geometries. After the geometric optimization of the three structures from the three codes, the three structures were used for a single-point calculation of the transmission with our NEGF-FIREBALL code. The resulting transmission plots are qualitatively the same with differences too small to be observed by an experimental measurement of conductance.

TABLE I. The bond lengths (angstrom) and the angles (degrees) of the armchair CNT with one oxygen atom (ether) attached on the orthogonal bond relaxed by DFT implemented in VASP and FIREBALL and a semiempirical model PM3 implemented in GAUSSIAN.

	VASP	GAUSSIAN	FIREBALL
C-C (orthogonal) (Å)	1.43	1.45	1.47
C-C (slanted) (Å)	1.43	1.44	1.46
C-C (ether) (Å)	2.09	2.12	2.15
C-O (ether) (Å)	1.39	1.41	1.41
∠C-O-C (ether) degrees	97.3	97.7	99.4
C-C (ether)/C-C (orthogonal)	1.47	1.47	1.47

TABLE II. The position as shown in Fig. 1, the relative energy, Δ, with respect to the total energy of two well separated ethers, the bond opening ratio, and the type of bond on the second oxygen atom where the first oxygen atom is attached as an ether on bond 1 of the armchair CNT.

Position	Δ (eV)	BOR	Second oxygen configuration
2	0.8	-	Physisorbed
3	1	1.11	Epoxide
4	−1.2	1.54	Ether, cooperative
5	1	1.11	Epoxide
6	0	1.48	Ether, noncooperative
7	1	1.11	epoxide

III. RESULTS AND DISCUSSION

A. Armchair study

There are two types of bonds on the armchair CNT on which a divalent atom such as oxygen can attach, orthogonal or slanted. The bonds are illustrated in Fig. 1. On an armchair CNT surface, oxygen attachment on the orthogonal bond (the bond in the circumferential direction perpendicular to the axis of the CNT such as bond 1 of Fig. 1) forms an ether in which two adjacent carbon atoms bond to the oxygen, and the original C-C bond is broken. The bond opening ratio is 1.47. Oxygen attachment on a slanted bond forms a three-membered ring known as epoxide in which the original C-C bond remains. The bond opening ratio is 1.11. The ether configuration is 1 eV more stable than the epoxide for our (7,7) CNT. The greater energetic stability of the ether compared to the epoxide has also been found by others.[10,15] Cho *et al.*[14] found that the energy difference between the epoxide and ether configurations becomes insignificant for higher diameter CNTs. We note that all of the above observations are consistent with the fact that epoxides are the spectroscopically identified configuration of oxidized flat graphite. Bonds in the axial direction of CNTs form epoxides as in flat graphite. Bonds in the circumferential direction which are strained by the curvature open up and form ethers.

1. Ether (orthogonal bond)

Since the ether configuration is more energetically stable than epoxide, we first investigate the energetics of a second oxygen addition to the single ether shown at bond 1 of Fig. 1. Since we are interested in cooperative addition, the energy of each configuration of two oxygen atoms is compared to the energy of two well-separated ethers. Denoting the energy of the configuration of interest as E_2 and the energy of two *well-separated* ethers as E_{2e}, we define the difference energy as $\Delta=E_2-E_{2e}$. Cooperative addition occurs when $\Delta<0$, otherwise it is *noncooperative*. Table II summarizes the relative

energy Δ, the bond opening ratio, and the type of bond formed when a second oxygen atom is attached.

Before discussing the various geometries of a second oxygen addition, it is instructive to consider the properties of a well-separated configuration of oxygen addends. When the oxygen atoms are well-separated, they act independently. This affects two different properties relevant to this study. The first property is the binding energy. The total binding energy of N well-separated oxygen atoms is N times the binding energy of one oxygen atom. Thus, every well-separated configuration is a noncooperative configuration. The second property is the electronic structure. For a well-separated distribution, the energy levels from the N oxygen atoms do not interact with each other. This is best illustrated by contrast. When oxygen atoms bind to a CNT within one or two C-C bonds of each other, the energy levels of the oxygen atoms interact and split and push up closer to the Fermi energy. This does not occur in well-separated configurations. While every well-separated configuration is a noncooperative configuration, a noncooperative configuration does not have to be a well-separated configuration. The terminology used to describe different configurations of oxygen addends will depend on the context of the discussion. If the focus is on the relative energetic stability of the configuration, configurations will be designated as either cooperative or noncooperative. The total energy of a well-separated configuration will always be used as the energy reference for describing the relative energies Δ of other configurations. If the focus is on the electronic structure, configurations will be designated as well-separated when appropriate.

Now, the energetics of a second oxygen addition to the single ether shown at bond 1 of Fig. 1 are described. With the first ether on bond 1 of Fig. 1, a second ether configuration can be obtained when an oxygen atom is placed on orthogonal bonds 4 or 6. Although bond 6 is only one slanted bond away from bond 1, the total energy with oxygen atoms on bonds 1 and 6 is the same as two isolated ethers, i.e., $\Delta=0$. When the second oxygen atom is placed on bond 4, $\Delta=-1.2$ eV, and cooperative addition occurs. With the second oxygen on bond 4, three carbon rings are affected (rings I–III). With the second oxygen on bond 6, four carbon rings are perturbed (rings I, II, IV, and V). Also when the second oxygen is placed at bond 4, the collective strain of the two oxygen atoms opens the C-C bond more than when the second oxygen atom is at bond 6. The bond opening ratio is 1.54 and 1.48 for oxygens at bond 4 and 6, respectively. These two effects combine to form the energetic stability at bond 4. This is the minimum energy configuration of two oxygen atoms on an armchair CNT, and we refer to it as a cooperative ether configuration. An oxygen atom on a slanted bond such as bond 3, 5, or 7 forms an epoxide, and $\Delta=1$ eV. The second atom can also attach at nearest-neighbor bond 2. When relaxed, the two oxygen atoms combine to form an oxygen molecule, and they no longer remain covalently attached to the CNT. The oxygen molecule is physisorbed on the CNT, and $\Delta=0.8$ eV. Thus, the most energetically favorable arrangement occurs when the oxygen atoms are on adjacent parallel bonds along the axial direction as shown in Fig. 2(a). The two oxygen atoms placed on parallel orthogonal bonds of the same carbon ring behave as cooperative ethers and minimize the total energy of the system.

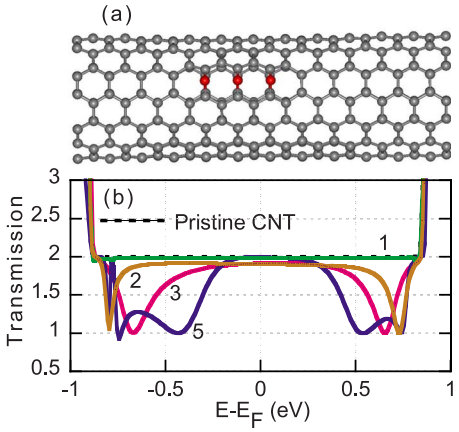

FIG. 2. (Color online) (7,7) CNT with a cooperative ether configuration of oxygen atoms in red on the orthogonal bonds repeated in the axial direction. (a) Relaxed structure with three cooperative ethers along the axial direction. (b) Transmission plots labeled according to the number of oxygen atoms. The transmission of the pristine CNT (dashed) is shown for comparison.

2. Cooperative ether (orthogonal bond)

After finding the cooperative ethers as the minimum energy configuration, we increase the number of oxygen atoms on parallel orthogonal bonds to form a line along the axial direction of the armchair CNT as shown in Fig. 2(a). The transmission plots of the structures with an increasing number of cooperative ethers are shown in Fig. 2(b). The transmission curve for one oxygen atom shows essentially no change from that of a pristine CNT within 1 eV of the Fermi level. With two oxygen atoms, the transmission plot shows a dip near the turn-on of the first excited modes about ± 0.75 eV away from the Fermi level. The width of this dip spreads in energy as we increase the number of atoms from 2 to 5. We observe that the cooperative addition pattern shown in Fig. 2 has a strong impact on the transmission symmetrically away from the Fermi level close to the turn on of the first excited modes, and the transmission near the Fermi level is relatively unaffected. This pattern has been observed by others and attributed to the fact that the oxygen states lie near the energies corresponding to the turn-ons of the bonding and anti-bonding first-excited modes.[11,15] We also find the oxygen states located near the energies of the first excited modes.

3. Noncooperative ether (orthogonal bond)

For comparison, we consider oxygen atoms placed on orthogonal bonds in a noncooperative fashion. The oxygen atoms are placed on the orthogonal bonds of a single atomic layer so that seven oxygen atoms form a complete ring around the CNT. Figure 3(a) shows the relaxed structure with three noncooperative ethers. The total energy of the structure with seven oxygen atoms is the same as that of seven well-separated ethers. The bond opening ratio is 1.48 in all the structures. Thus this configuration has no additional stability

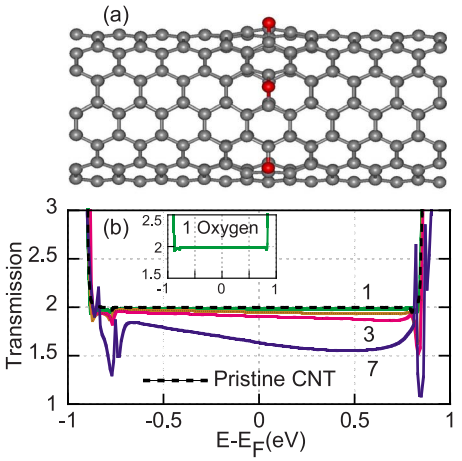

FIG. 3. (Color online) (7,7) CNT with a noncooperative ether configuration of oxygen atoms in red on the orthogonal bonds repeated in the circumferential direction. (a) Relaxed structure with three noncooperative oxygen atoms. (b) Transmission plots labeled according to the number of oxygen atoms (plot for two oxygen atoms lies between 1 and 3). The dashed line is the transmission of the pristine CNT shown for comparison. Inset: transmission with one oxygen atom.

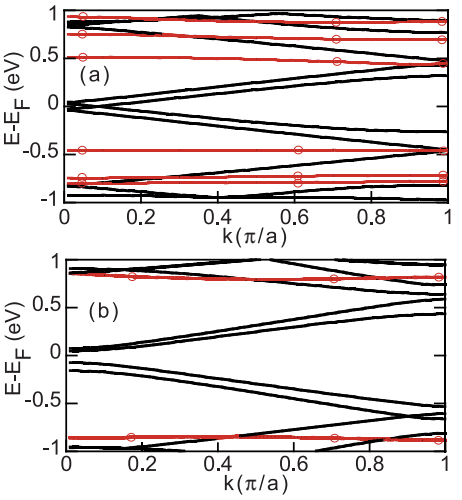

FIG. 4. (Color online) *E-k* plot of (7,7) CNT with oxygen atoms on the orthogonal bonds. (a) Five cooperative oxygen atoms with configuration and supercell length as shown in Fig. 2 and (b) seven well-separated oxygen atoms with configuration and supercell length as shown in Fig. 3. The black lines are the CNT bands resulting from its constituent carbon atoms. The red circled, horizontal lines indicate localized states resulting from the oxygen atoms.

other than that obtained by the isolated ether formation.

Figure 3(b) shows the transmission for one, two, three, and seven oxygen atoms. The transmission for a single oxygen atom is the same as in Fig. 2, and it is also shown in the inset for clarity. For two or three oxygen atoms, the dip in transmission at the turn-on of the first-excited modes is significantly reduced in magnitude and narrower in energy than the dips resulting from the cooperative axial addition of Fig. 2. With seven oxygen atoms which circle the CNT on every orthogonal bond in a single atomic layer, the transmission is reduced by 20% at the Fermi level and the dips at the first-excited modes are still small and narrow compared to those resulting from the cooperative addition along a set of parallel, orthogonal bonds. This is an indication that the oxygen atoms are well-separated.

4. Cooperative versus well-separated electronic structure

To elucidate the effect on transmission of cooperative versus well-separated addition, we consider the energy versus wave vector (*E-k*) relations of the two different supercells corresponding to the addition patterns shown in Figs. 2 and 3, respectively. The lengths of the supercells are as shown in Figs. 2 and 3. For cooperative addition, we use the structure of Fig. 2 with five oxygen atoms. For well-separated addition, we use the structure of Fig. 3 with seven oxygen atoms. The *E-k* plots for cooperative and well-separated addition are shown in Figs. 4(a) and 4(b), respectively. The circled, horizontal lines indicate localized states resulting from the oxygen atoms. Comparing Figs. 4(a) and 4(b), one observes that for cooperative addition, a splitting of the localized states occurs with some of the localized states pushed closer to the Fermi energy. Comparing the *E-k* plots with the corresponding transmission plots shown in Figs. 2 and 3, one observes that the oxygen energy levels are coincident with a dip in transmission at the corresponding energies. Thus, cooperative addition gives rise to a larger interaction among the oxygen atoms, splitting the levels and pushing them closer to the Fermi level. This, in turn, gives rise to the wider and multiple dips in transmission that move closer to the Fermi level as atoms are added in a cooperative manner.

5. Cooperative epoxide (slanted bond)

So far, we have considered oxygen addition on the orthogonal bonds. Now, we consider oxygen addition on the slanted bonds. A single oxygen atom attaches on one of the slanted bonds such as bond 3, 5, or 7 of Fig. 1 as an epoxide. Although the energy of an epoxide is 1 eV higher than that of an ether, there has been a DFT-based prediction of a chemical route to epoxidation of a CNT sidewall.[39] We investigate if there is any cooperative effect that could minimize the energy of the system when multiple oxygens are attached in the epoxide configuration at close proximity.

When the oxygen atom forms an epoxide, the C-C bond associated with the ring is slightly stretched. When three oxygen atoms are placed on adjacent parallel bonds, their collective strain becomes large enough to open the C-C bond completely at middle position 2 (Fig. 5(a)) and partially at positions 1 and 3. The bond opening ratios are 1.18 and 1.48 for positions 1 and 2, respectively. Thus, the middle oxygen atom forms an ether sandwiched by two epoxides. The energy of the system reduces by 1 eV for each bond cleavage. Such bond cleavage and energy minimization can occur only when the oxygen atoms are placed on adjacent parallel slanted bonds which we call the cooperative epoxide configuration. This is similar to the oxygen driven unzipping of graphitic material predicted by Li *et al.*[19] As more oxygen atoms are added, the total energy of the system becomes

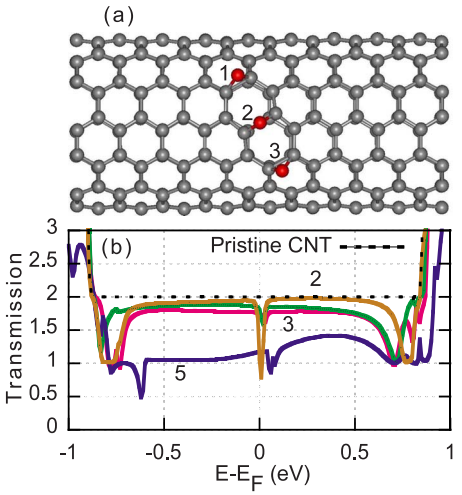

FIG. 5. (Color online) (7,7) CNT with cooperative epoxide oxygen atoms on the slanted bonds repeated in the spiral direction. (a) Relaxed structure with three cooperative epoxide oxygen atoms. (b) Transmission plots labeled according to the number of oxygen atoms.

comparable to the additive total energy obtained from an equal number of well-separated ethers shown in Fig. 3(a). For example, the configuration with five oxygen atoms on adjacent, slanted bonds results in three ethers sandwiched by two epoxides. The bond opening ratios are 1.15, 1.57, and 1.62 from the end to the middle oxygen atom. This cooperative epoxide configuration of five oxygen atoms is 3 eV lower in energy than five well-separated epoxides, 2 eV higher in energy than five well-separated ethers, and 5 eV higher in energy than five cooperative ethers along the axial direction shown in Fig. 2(a).

Figure 5(b) shows the corresponding transmission plots of the armchair CNT sequentially functionalized by oxygen atoms on adjacent, parallel, slanted bonds. A single epoxide oxygen has a more pronounced effect on the transmission both at and away from the Fermi level compared to that of a single ether oxygen addition. The transmission at the Fermi level is lowered by about 15%. In contrast, the transmission at the Fermi level is unaffected by a single oxygen in the ether configuration. With three oxygen atoms the transmission is essentially similar to and slightly reduced from the single atom case. With five oxygen atoms, however, the transmission is significantly affected. This is because with five atoms, at least three bonds are completely open and it perturbs the local geometry of the CNT. In the slanted bond configuration, when the bond opens, the length of the unit cell increases at the functionalized region and it perturbs the other nonfunctionalized unit cells along the length of the CNT. On the other hand, opening of an orthogonal bond does not affect the axial length of the unit cell locally and the adjacent unit cells remain unperturbed by such bond cleavage. Thus, although more than one oxygen atom on adjacent, parallel, slanted bonds cleave the C-C bonds and result in ethers; the transmission at the Fermi level is affected more than that from a comparable number of ethers on orthogonal bonds such as shown in Figs. 2 and 3.

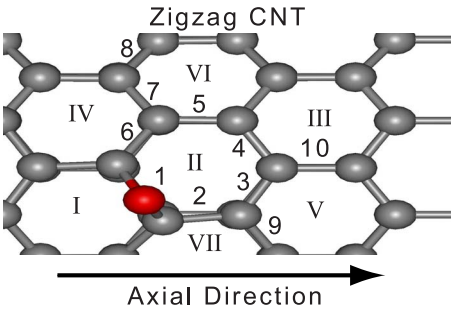

FIG. 6. (Color online) Section of a zigzag CNT illustrating the two types of bonds, axial and slanted. Arabic numerals label the bonds and Roman numerals label the rings. The red atom at bond 1 is the oxygen atom. "Axial" denotes the bonds that are parallel to the axial direction such as bonds 2 and 5. Slanted denotes the other type of bond such as 4 and 7.

B. Zigzag study

Following the armchair CNT study, we investigate the effect of adjacent oxygen attachment on the transmission of a metallic zigzag CNT. There are two types of bonds on the zigzag CNT, axial and slanted. The bonds are illustrated and defined in Fig. 6. Relative energetic stability of these configurations has been debated in many cases where some studies favor the axial connection to be more stable,[32,40,41] and other studies find the slanted geometry more stable.[10] Using a (8,0) CNT Dag *et al.*[12] found the slanted configuration to be stable only by 0.02 eV. On the other hand, using the same CNT Chen *et al.*[10] found the slanted configuration to be stable by 1.11 eV. Cho *et al.*[14] found for (9,0) tubes the slanted configuration to be 0.18 eV lower in energy than the axial configuration using a dichlorocarbene (divalent) addend. We find that the energy of the slanted bond configuration is 0.9 eV lower than the energy of the axial bond configuration and that the bond opening ratios of the slanted and axial configurations are 1.21 and 1.09, respectively. Thus, on a zigzag CNT surface, oxygen attachment on the slanted bond forms an ether, and oxygen attachment on the axial bond forms an epoxide. Again, our results are consistent with the fact that epoxides are the spectroscopically identified configuration on oxidized flat graphite. Bonds primarily in the axial direction of CNTs form epoxides as in flat graphite. Bonds in the circumferential direction which are strained by the curvature open up and form ethers. Note that the magnitude of the bond opening ratio is lower in a zigzag CNT compared to that of an armchair CNT. This is expected since the orthogonal bonds on an armchair CNT are more strained than the slanted bonds of the zigzag CNT.

1. Ether (slanted bond)

Since ether is more energetically stable than epoxide, we first investigate the energetics of a second oxygen addition to the single ether shown at bond 1 of Fig. 6. Table III summarizes the relative energy Δ, the bond opening ratio, and the type of bond formed when a second oxygen atom is attached. Denoting the energy of the configuration of interest as E_2 and the energy of two isolated ethers on the zigzag CNT as E_{2e}, we define the difference energy as $\Delta = E_2 - E_{2e}$. With the first

TABLE III. The position as shown in Fig. 6, the relative energy Δ with respect to the total energy of two well separated ethers, the bond opening ratio, and the type of bond on the second oxygen atom where the first oxygen atom is attached as an ether on bond 1 of the zigzag CNT.

Position	Δ (eV)	BOR	Second oxygen configuration
2			Goes to bond 9 and forms ether
3	−1.5	1.48	Ether, cooperative
4	−2	1.54	Ether, cooperative
5	1	1.09	Epoxide
6	0.8	1.16	Partial epoxide and ether
7	0	1.18	Ether, noncooperative
8	0	1.21	Ether, noncooperative

oxygen atom placed on slanted bond 1, a second ether configuration can be obtained when an oxygen atom is placed on the slanted bond at 3, 4, or 7 (Fig. 6). Bond 7 is one slanted bond away from the first atom and bonds 3 and 4 are two slanted bonds away. The relative energies, Δ, for the second oxygen attached at bonds 3, 4, and 7 are −1.5, −2.0, and 0 eV, respectively. With the second oxygen on bond 7, four carbon rings are perturbed (rings I, II, V, and VI). With the second oxygen on bonds 3 or 4, three carbon rings are affected (rings I, II, and V or rings I–III, respectively). Also when the second oxygen is placed at bond 4, the collective strain of the two oxygen atoms opens the C-C bond more than when the second oxygen atom is at bond 7 or bond 3. The bond opening ratios are 1.48, 1.54, and 1.18 for oxygen atoms on bonds 3, 4, and 7, respectively. These two effects combine to give the greatest energetic stability to a second oxygen attachment at bond 4. We term this configuration of two oxygens on parallel slanted bonds of a six-sided ring as cooperative ether on a zigzag CNT. A nearest-neighbor attachment can occur if the second oxygen attaches at bond 2 or 6. When the second oxygen is attached on bond 2, upon relaxation it moves to bond 9. In this case, the strains on the C-C bond exerted by the two oxygen atoms oppose each other. Hence the two oxygen atoms form epoxides with a bond opening ratio of 1.11. When the second oxygen atom is placed on bond 6, the oxygen atom at 1 forms ether with a bond opening ratio of 1.54 and the oxygen atom on bond 6 forms a partial epoxide with a bond opening ratio of 1.16. The relative energies with oxygens at bonds 6 and 9 are $\Delta = 0.8$ eV and $\Delta = 1.9$ eV, respectively. A second oxygen atom on an axial bond such as bond 5 or 10 forms an epoxide with a relative energy of $\Delta = 1$ eV. Thus, the most energetically favorable arrangement occurs when the oxygen atoms are on adjacent parallel bonds along the spiral direction as shown in Fig. 7(a). As more oxygen atoms are placed consecutively along the spiral line, their cooperative effect increases their relative energetic stability compared to any other adduct configuration. The cooperative ethers on a zigzag CNT form a spiral line when the number of oxygen atoms is increased.

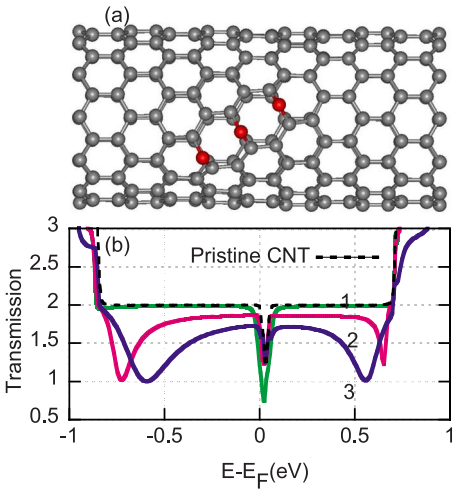

FIG. 7. (Color online) (12,0) CNT with cooperative ether configuration oxygen atoms on the slanted bonds repeated in the spiral direction. (a) Relaxed structure with three cooperative oxygen atoms. (b) Transmission plots labeled according to the number of oxygen atoms.

2. Cooperative ether (slanted bond)

The transmission corresponding to the spiral cycloaddition is shown in Fig. 7(b). For one oxygen, the transmission is essentially unchanged from the transmission of the pristine CNT. We only see the intrinsic transmission dip at the Fermi level resulting from the small band gap of a pristine zigzag (12,0) CNT. There is a dip in transmission above the first-excited modes which falls outside of the plot. When a second oxygen is added, a dip in transmission occurs at the turn-on of the first-excited mode. As more oxygen atoms are added, the dip deepens and broadens and lowers the transmission of the fundamental mode over a wider range of energy. The origin of this transmission dip is due to the orbital energy level splitting of adjacent oxygen atoms similar to the cooperative oxygen addition on an armchair CNT discussed in reference to Fig. 4. At the Fermi level, the transmission and hence the zero bias conductance drops by 10% when three oxygen atoms are attached.

3. Noncooperative ether (slanted bond)

For comparison, we sequentially add oxygen atoms to alternating slanted bonds in the circumferential direction in a noncooperative ether configuration as shown in Fig. 8(a). As before, the oxygens bond as ethers. The transmissions of the two structures shown in Figs. 8(a) and 7(a) are essentially the same. This similarity is a result of the comparable distance between the oxygen atoms in the two configurations. The proximity of oxygen atoms causes mixing and a splitting of the oxygen states moving them closer to the Fermi level. Hence the transmission dip broadens and shifts toward the Fermi level with increasing number of oxygen additions. This is an example of a noncooperative configuration that is not well-separated.

4. Cooperative (axial bonds)

The axial bonds are the least energetically favorable for oxygen addition; however, we consider their cooperative be-

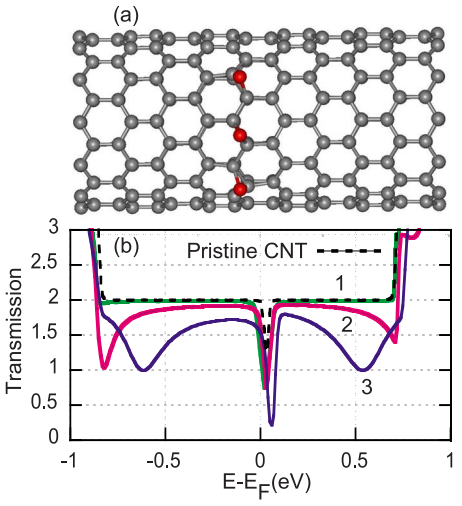

FIG. 8. (Color online) (12,0) CNT with a noncooperative ether configuration of oxygen atoms on the slanted bonds repeated in the circumferential direction. (a) Relaxed structure with three noncooperative oxygen atoms. (b) Transmission plots labeled according to the number of oxygen atoms.

havior and the effect on transmission. Figure 9(a) shows the relaxed structure of a (12,0) CNT with oxygen atoms attached on the axial bonds. The number of oxygen atoms is increased sequentially on adjacent axial bonds around the circumference of the CNT. One oxygen on the axial bond of a zigzag CNT forms an epoxide with a bond opening ratio of 1.09. Similar to the slanted bond configuration on an armchair CNT shown in Fig. 5(a), when three atoms are placed adjacently, their collective strain becomes large enough to open the C-C bond completely at the middle position and partially at two side positions as shown in Fig. 9(a). The bond opening ratio is 1.13 for the side bonds and 1.5 for the middle bond. Thus the middle oxygen atom forms an ether sandwiched by two epoxides. The overall energy of the system reduces by 1 eV for each bond cleavage. When the CNT is completely wrapped by 12 oxygens, all the bonds open to form 12 ethers. The bond opening ratio is 1.55, the energy is 12 eV lower than the energy of 12 well-separated epoxides, and it is equal to the energy of 12 well-separated ethers.

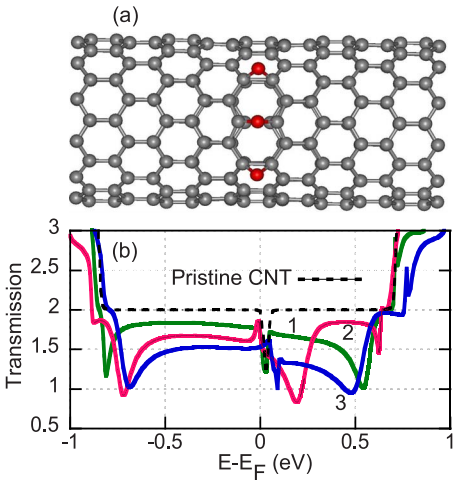

FIG. 9. (Color online) (12,0) CNT with cooperative epoxide oxygen atoms on the axial bonds repeated in the circumferential direction. (a) Relaxed structure with three cooperative epoxide oxygen atoms. (b) Transmission plots labeled according to the number of oxygen atoms.

The transmission value decreases by about 10% on either side of the dip at the Fermi level when one oxygen atom is attached. Similar to the armchair slanted bond configuration (Fig. 5), as the number of oxygen atoms is increased, bond cleaving occurs which increases the length of the unit cell in the functionalized region and perturbs the adjacent rings. The intrinsic dip in transmission seen in Figs. 8(a) and 7(a) is missing for more than one oxygen addition. Because of this, the transmission right at the Fermi level is higher in this configuration than in the slanted configuration, and on either side of the dip it is lower. The configurations of Figs. 7(a) and 9(a) result in comparable zero-bias conductances. If 12 oxygen atoms are wrapped entirely around the CNT in Fig. 9(a), the CNT is cut into two pieces connected by the 12 ethers formed by the 12 oxygen atoms. This results in a conductance drop of 3 orders of magnitude which is the largest drop that we observe for any configuration.

Summarizing the results from the armchair and zigzag CNT studies, ether-type oxygen attachment is energetically favorable compared to epoxide attachment on both the armchair and zigzag CNTs. Ether-type bonding occurs on the orthogonal bond of an armchair CNT and the slanted bond of a zigzag CNT. In both cases, ethers placed on the adjacent parallel bonds of the six-membered carbon ring are the energetically most favorable configuration. These configurations which we call cooperative ethers are the most probable candidates for a clustered addition topography. The levels of the isolated oxygen atoms occur near the turn-on of the first excited modes above and below the Fermi level. Clustered addition with oxygen atoms in close proximity results in a splitting of the oxygen levels which pushes them closer to the Fermi level. As the levels move closer to the Fermi level, transmission at the Fermi level is reduced.

C. Metal to semiconductor transition

Experimentally, one or several localized molecular attachments on a CNT were shown to change the conductance versus gate voltage response of metallic CNTs to resemble that of *p*-type semiconducting CNTs.[5] In an effort to understand this result, we investigate additional patterns that could cause the conductance of a metallic CNT to resemble the conductance of a semiconducting CNT. Previous DFT calculations with divalent adatoms have concentrated on a random distribution to study metal to nonmetal transition behavior.[11,14,15,17] Guided by the experimental procedure, we investigate the effect of a few atoms clustered in a localized region. We look for quasigaps in the transmission spectra and actual gaps in the supercell E versus k relations.

1. Armchair cooperative ether cluster

From the results presented above, we observe that the transmission is more strongly affected when the oxygen atoms are placed close together as in a cooperative manner

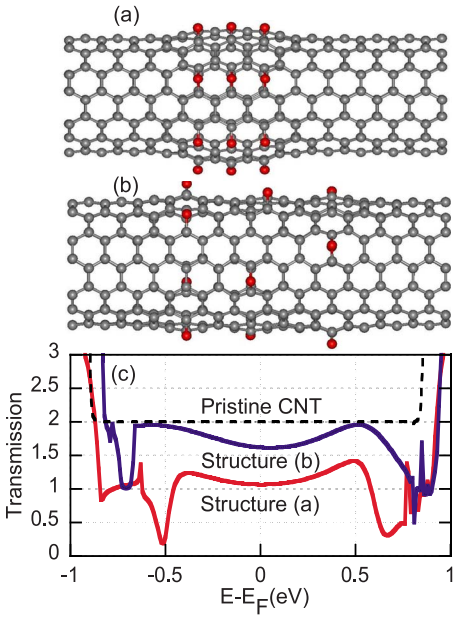

FIG. 10. (Color online) (7,7) CNT with 12 oxygen atoms (red) attached in ether configuration on the orthogonal bonds. (a) Relaxed structure with 12 cooperative oxygen atoms. (b) Relaxed structure with 12 well-separated oxygen atoms. (c) Transmission plot for cooperative (red) and well-separated (blue) oxygen atoms.

compared to a well-separated distribution. To further investigate this trend, we simulate 12 oxygens on an armchair CNT in a cooperative configuration [Fig. 10(a)] and in a well-separated configuration [Fig. 10(b)]. The cooperative configuration consists of four rows of three oxygen atoms on alternating axial lines. The most dense functionalization on the orthogonal bonds of an armchair CNT would occur when *adjacent* axial lines are functionalized. However, this is not an energetically favorable configuration. Using the energy, E_{12e}, of a 12 well-separated ether configuration as the reference, the relative energy of the alternating configuration of Fig. 10(a) is −5 eV, and the relative energy of the adjacent configuration is +4 eV.

Figure 10(c) shows the corresponding transmission plots for the cooperative [structure (a)] and well-separated [structure (b)] configurations. The well-separated configuration results in less change in the transmission compared to the cooperative configuration. At the Fermi level, the transmission is reduced by 20% for the well-separated configuration and by 50% for the cooperative configuration. Although significant transmission modulation is observed for cooperative addition at 0.5 eV away from E_f, conductance remains robust over a 1 eV energy range close to the Fermi level. Thus, it is unlikely that localized addition on the armchair CNT can cause a metal to semiconductor transition. Hence we investigate the effect of similar addition configurations on the zigzag CNT.

2. Zigzag cooperative ether cluster

We model 16 oxygen atoms on the slanted bonds of a zigzag CNT surface in one well-separated and two cooperative configurations shown in Figs. 11(a) and 11(b). The cooperative configurations consist of spiral lines of oxygen atoms. In Fig. 11(a), alternating spiral lines are functionalized, and the oxygen atoms extend over the entire circumference of the CNT. In Fig. 11(b), adjacent spiral lines are functionalized, and the oxygen atoms are on the top half of the CNT. In both cases, the four interior spiral lines consist of three oxygen atoms, and the outer two lines consist of two oxygen atoms. Oxygen atoms on alternating spiral lines result in the most energetically favorable configuration as in the armchair case [Fig. 10(a)]. The atoms form ethers and the bond opening ratios are 1.52 and 1.60 for the edge and middle oxygen atoms, respectively. Using the energy E_{16e} of the 16 well-separated ether configuration as the reference, the relative energy of the alternating spiral arrangement is −6 eV, and the relative energy of the adjacent spiral arrangement is 0 eV. The well-separated and the adjacent spiral configurations result in equal total energies. This contrasts with the armchair

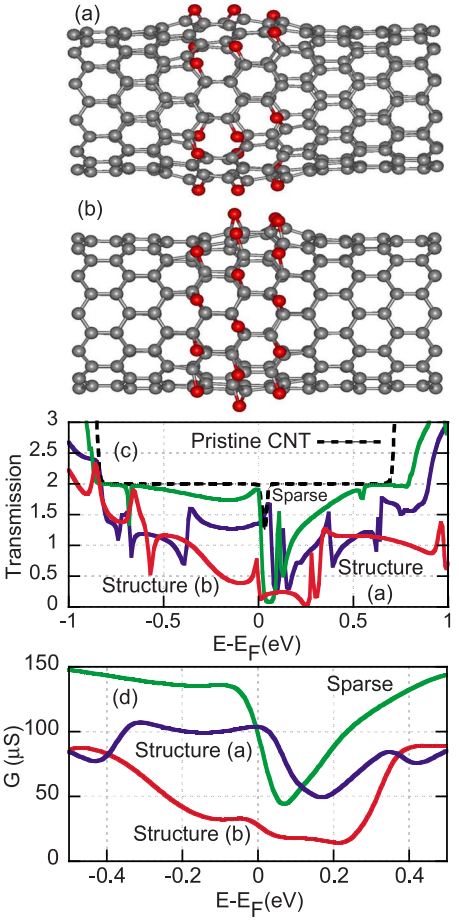

FIG. 11. (Color online) (12,0) CNT with 16 oxygen atoms on the slanted bonds on the upper surface. (a) Structure of parallel spiral lines each containing three O atoms with one row gap between them (cooperative alternating). (b) Structure of parallel spiral lines each containing three O atoms with no gap or 16 clustered O atoms (cooperative adjacent). (c) Transmission plot for cooperative clustered (red online), cooperative one row gap (blue online) and well-separated (labeled as "sparse") (green online) oxygen distributions. (d) Conductance versus E_f of the cooperative clustered (red online), cooperative one row gap (blue online) and well-separated (labeled as sparse) (green online) oxygen distributions.

case in which the energy of the adjacent axial configuration is 4 eV higher than the energy of the well-separated configuration. The oxygens bond as ethers along a single spiral line. When adjacent spiral lines are functionalized as in Fig. 11(b), the ethers begin to close. With multiple adjacent spiral lines, the oxygen atoms that are in the middle region form epoxides which are sandwiched by ethers on the two edges in the circumferential direction. The bond opening ratio is 1.08 for the epoxides and 1.51 for the ethers. Thus, on a zigzag CNT surface, a clustered configuration such as Fig. 11(b) results in epoxides that are as energetically stable as an equal number of ethers in an well-separated arrangement.

Figure 11(c) shows the corresponding three transmission plots of 16 oxygen atoms on a zigzag CNT. The transmissions of all the structures show a significant drop immediately above the Fermi level. Also the transmission is asymmetric with respect to the Fermi level. The dip in the transmission of the adjacent spiral configuration [structure (b)] is broader and deeper than that of the well-separated (sparse) and alternating cooperative spiral configuration [structure (a)], and, overall, the transmission of the adjacent spiral configuration is lower. An *E-k* calculation of the supercell of the adjacent spiral configuration shown in Fig. 11(b) shows that an energy gap of about 300 meV opens immediately above the Fermi level. The gap opens at the charge neutral point of the pristine CNT. The oxygen atoms lower the Fermi level of the functionalized CNT with respect to that of the pristine CNT. This gives rise to an asymmetry of the transmission with respect to the Fermi level of the functionalized CNT.

The corresponding conductance versus E_f curves of the three structures are plotted in Fig. 11(d). All curves decrease to a minimum above the charge-neutral Fermi level and then increase at higher energies returning back to their starting value. The conductance of the well-separated distribution (green color online) is, overall, the highest in magnitude. The adjacent spiral configuration results in the minimum conductance and largest modulation of conductance. The conductance of this configuration (red color online) drops 80% from 90 μS at $E_f-0.5$ eV to a minimum of 17 μS at $E_f+0.2$ eV at which point it begins to rise back to its original value.

There are both similarities and differences between this conductance curve and those observed experimentally.[5] The drop in conductance with increasingly positive Fermi energy is qualitatively similar to that observed experimentally with increasingly positive gate bias shown in Fig. 2 of Ref. 5. There is the usual large difference in the voltage/energy scale since the experimental gate voltage is applied with a back gate. The experimental gate voltage sweeps the Fermi level over a fraction of the 1.0 eV range. Also the CNTs are charged during the experiment and the Fermi energy is more negative consistent with *p*-type doping. Finally, we note that the relatively large modification of the conductance is the result of 16 oxygen atoms locally grouped on a zigzag CNT. For a single oxygen atom, either ether or epoxide, on either a (7,7) or (12,0) CNT, we find no configuration that would lead to a significant change in conductance, or, in particular, a notably asymmetric conductance with respect to the Fermi energy.

IV. SUMMARY

In summary, we have modeled the geometry and transmission of metallic (7,7) and (12,0) CNTs with a few grouped and ungrouped covalently attached oxygen atoms. We find that oxygen atoms attached on the CNT surface within the same carbon ring on parallel bonds are energetically more stable than well-separated attachments. In an armchair CNT, oxygen attachment favors orthogonal, ether bonding, and it is energetically favorable when propagating in the axial direction of the CNT. In a zigzag CNT, oxygen attachment prefers the slanted bond and is energetically favorable when propagating spirally through the length of the CNT. For both armchair and zigzag CNTs, closely spaced oxygen attachment on the CNT surface causes a dip in transmission symmetrically away from the Fermi level near the turn-ons of the first-excited modes. As more oxygen atoms are placed in close proximity, their levels interact and split and move closer to the Fermi level which results in broader dips in transmission closer to the Fermi level. When multiple adjacent spiral lines of a zigzag CNT are functionalized, the ether bonds on the inside lines transform to epoxides with ethers remaining along the edge of the cluster. The total energy of this type of cluster is equal to the energy of an equal number of well-separated ether attachments. This type of clustered addition can result in a gap opening in the transmission centered around the charge neutral point of the pristine zigzag CNT. The oxygen atoms lower the Fermi level of the functionalized CNT which results in an asymmetry of the transmission with respect to the Fermi level of the functionalized CNT. This results in a conductance versus Fermi energy curve that shows a qualitative resemblance to conductance versus gate bias curves observed experimentally. A single oxygen adatom in any configuration on either a (7,7) or (12,0) metallic CNT does not give rise to the large change in conductance asymmetric with respect to the Fermi level that is observed experimentally.[5]

ACKNOWLEDGMENTS

This work is supported by the Microelectronics Advanced Research Corporation Focus Center on Nano Materials (FENA) and the NSF (Contract No. ECS-0524501). We thank V. Lordi for providing support and training for running the VASP simulations at Lawrence Livermore National Laboratory. It is a pleasure to thank B. R. Goldsmith for sharing experimental data and helpful discussions. M.K.A. thanks Z. Chen and T. Yumura for helpful discussions regarding cooperative addition.

*mashraf@ee.ucr.edu
†nbruque@ee.ucr.edu

[1] B. R. Goldsmith, J. G. Coroneus, A. A. Kane, G. A. Weiss, and P. G. Collins, Nano Lett. **8**, 189 (2008).
[2] K. Besteman, J. O. Lee, F. G. M. Wiertz, H. A. Heering, and C. Dekker, Nano Lett. **3**, 727 (2003).
[3] J. Kong, N. R. Franklin, C. W. Zhou, M. G. Chapline, S. Peng, K. J. Cho, and H. J. Dai, Science **287**, 622 (2000).
[4] K. Galatsis, R. Potok, and K. L. Wang, IEEE Trans. Semicond. Manuf. **20**, 542 (2007).
[5] B. R. Goldsmith, J. G. Coroneus, B. R. Khalap, A. A. Kane, G. A. Weiss, and P. G. Collins, Science **315**, 77 (2007).
[6] Y. Fan, B. R. Goldsmith, and P. G. Collins, Nature Mater. **4**, 906 (2005).
[7] J. Chen, M. A. Hammon, H. Hu, Y. Chen, A. M. Rao, P. C. Eklund, and R. C. Haddon, Science **282**, 95 (1998).
[8] K. Kamaras, M. E. Itkis, H. Hu, B. Zhao, and R. C. Haddon, Science **301**, 1501 (2003).
[9] H. Hu, B. Zhao, M. A. Hammon, K. Kamaras, M. E. Itkis, and R. C. Haddon, J. Am. Chem. Soc. **125**, 14893 (2003).
[10] Z. Chen, S. Nagase, A. Hirsch, R. C. Haddon, W. Thiel, and P. R. Schleyer, Angew. Chem., Int. Ed. **43**, 1552 (2004).
[11] H. Park, J. Zhao, and J. P. Lu, Nano Lett. **6**, 916 (2006).
[12] S. Dag, O. Gülseren, T. Yildirim, and S. Ciraci, Phys. Rev. B **67**, 165424 (2003).
[13] S. Ciraci, S. Dag, Y. Yildirim, O. Gülseren, and R. T. Senger, J. Phys.: Condens. Matter **16**, R901 (2004).
[14] E. Cho, H. Kim, C. Kim, and S. Han, Chem. Phys. Lett. **419**, 134 (2006).
[15] Y. S. Lee and N. Marzari, Phys. Rev. Lett. **97**, 116801 (2006).
[16] H. Park, J. Zhao, and J. P. Lu, Nanotechnology **16**, 635 (2005).
[17] J. Zhao, Z. Chen, Z. Zhou, H. Park, P. R. Schleyer, and J. P. Lu, ChemPhysChem **6**, 598 (2005).
[18] T. Yumura and M. Kertesz, Chem. Mater. **19**, 1028 (2007).
[19] J.-L. Li, K. N. Kudin, M. J. McAllister, R. K. Prud'homme, I. A. Aksay, and R. Car, Phys. Rev. Lett. **96**, 176101 (2006).
[20] M. Bockrath, W. Liang, D. Bozovic, J. H. Hafner, C. M. Lieber, M. Tinkham, and H. Park, Science **291**, 283 (2001).
[21] O. F. Sankey and D. J. Niklewski, Phys. Rev. B **40**, 3979 (1989).
[22] A. A. Demkov, J. Ortega, O. F. Sankey, and M. P. Grumbach, Phys. Rev. B **52**, 1618 (1995).
[23] O. F. Sankey, A. A. Demkov, W. Windl, J. H. Fritsch, J. P. Lewis, and M. Fuentes-Cabrera, Int. J. Quantum Chem. **69**, 327 (1998).
[24] J. P. Lewis, K. R. Glaesemann, G. A. Voth, J. Fritsch, A. A. Demkov, J. Ortega, and O. F. Sankey, Phys. Rev. B **64**, 195103 (2001).
[25] P. Jelinek, H. Wang, J. P. Lewis, O. F. Sankey, and J. Ortega, Phys. Rev. B **71**, 235101 (2005).
[26] N. A. Bruque, R. R. Pandey, and R. K. Lake, Phys. Rev. B **76**, 205322 (2007).
[27] J. L. Martins, N. Troullier, and S. H. Wei, Phys. Rev. B **43**, 2213 (1991).
[28] A. D. Becke, Phys. Rev. A **38**, 3098 (1988).
[29] C. Lee, W. Yang, and R. G. Parr, Phys. Rev. B **37**, 785 (1988).
[30] J. Harris, Phys. Rev. B **31**, 1770 (1985).
[31] W. M. C. Foulkes and R. Haydock, Phys. Rev. B **39**, 12520 (1989).
[32] D. C. Sorescu, K. D. Jordan, and P. Avouris, J. Phys. Chem. B **105**, 11227 (2001).
[33] J. A. Steckel, K. D. Jordan, and P. Avouris, J. Phys. Chem. A **106**, 2572 (2002).
[34] M. J. Frisch *et al.*, GAUSSIAN 03, Revision D.01 (2003), Gaussian, Inc., Wallingford, CT, 2004.
[35] G. Kresse and J. Hafner, Phys. Rev. B **48**, 13115 (1993).
[36] J. Stewart, J. Comput. Chem. **10**, 209 (1989).
[37] J. Stewart, J. Comput. Chem. **10**, 221 (1989).
[38] J. P. Perdew, K. Burke, and M. Ernzerhof, Phys. Rev. Lett. **77**, 3865 (1996).
[39] X. Lu, Q. Yuan, and Q. Zhang, Org. Lett. **5**, 3527 (2003).
[40] S. P. Chan, G. Chen, X. G. Gong, and Z. F. Liu, Phys. Rev. Lett. **90**, 086403 (2003).
[41] D. J. Mann and M. D. Halls, J. Chem. Phys. **116**, 9014 (2002).